Proceedings of the 51^{st} Hawaii International Conference on System Sciences | 2018

Location-Dependent Impacts of Resource Inertia on Power System Oscillations

Ti Xu , Wonhyeok Jang, Thomas Overbye
Department of Electrical and Computer Engineering
Texas A&M University, College Station, TX, USA
{txu, wjang777, overbye}@tamu.edu

Abstract

Inertial responses are seen by the system as the injection or withdrawal of electrical energy, corresponding to a change of frequency. The inertia of a machine primarily contributes to the power system transient stability. Oscillations are always present in the bulk power system due to the electromechanical nature of the grid. Poorly damped oscillations may cause system instability. Thus, this paper aims to study inertia's impacts on system primary frequency response, in particular on system oscillation modes. Both transient stability simulations and modal analysis are performed to provide insights into the extent to which inertia and its location influence the system oscillation behavior. Simulation results using both a small-scale test system and a large-scale synthetic network dynamic model are presented to verify the locational impacts of resource inertia.

1. Introduction

Primary frequency response (PFR) is largely determined by generators' inertia and governor responses. As the power system generation side is changing to include more renewable resources connected by power electronics and more light-weight generators, the system is shifting towards less inertia. With lower grid inertia, small events may result in larger frequency excursions than before. Reports [1], [2] by the North American Electric Reliability Corporation (NERC) indicated a declining frequency response in both the Eastern Interconnection (EI) and the Electric Reliability Council of Texas (ERCOT) footprints. In references [3], [4], authors performed time-domain simulations to analyze the inertia's impacts on transient stability. Previous work [5] investigated the location-dependent impacts of inertia on power system primary frequency response.

Post-disturbance system oscillation modes are of interest for evaluating the system transient stability, in addition to minimum/maximum rate of change of frequency (RoCoF) and minimum/maximum frequency during the first several seconds after disturbances. Power systems can experience a wide range of oscillations, ranging from high-frequency switching transients to sustained low frequency ($<$ 2 Hz) inter-area oscillations affecting an entire interconnect. A system oscillation mode is a natural property of electromechanical system, and characterized by its oscillating frequency, damping performance and effect area [6]. An oscillation can be either undamped, positively damped (decaying with time) or negatively damped (growing with time). However, there are few works studying the impacts of resource inertia on system oscillation frequency and damping behavior. Modal analysis was used in [7] for analysing phase angle-based power system inter-area oscillation. Works [8], [9] applied modal analysis for studies on inertia in consideration of deep solar energy penetration. Authors also extracted modal information to investigate damping of inter-area oscillations in large interconnected power systems [10].

As such, we aim to investigate how system oscillation modes vary with inertia being reduced and how this oscillation mode variation is related to inertia's location. This paper first uses a straight-forward small-scale test system for illustration. To obtain realistic simulation results, this paper also performs studies on a large-scale synthetic network model [11]–[14]. A set of scenarios with various inertia at different sites are constructed to show, for a power system, what aspects the inertia and its location have effects on. The test system in some cases experiences natural oscillations, and forced ones in other cases. In this work, we focus on local plant oscillations. The major effect area of the local plant oscillation is localized to a small set of generators close to each other and lines connecting them [15]. Specifically, we perform time-domain simulations and modal analysis for inertia studies.

In this paper, four more sections come as follows. Section II provides some background knowledges on transient stability formulation and modal analysis techniques. In Section III, a simple example is applied to illustrate inertia's locational impacts. Simulations results on a large-scale synthetic system model with varying regional inertia are presented in Section IV. Conclusion and future work direction are provided in Section V.

URI: http://hdl.handle.net/10125/50230
ISBN: 978-0-9981331-1-9

2. Background

In this section, we give an overview of transient stability formulation and the role of inertia in the formation. We also briefly discuss about the basic idea of all techniques to extract power system modal information.

2.1. The Machine Swing Equation in System Transient Stability Formulation

To determine response of the system over a time period of seconds to perhaps a minute after a contingency, a set of differential and algebraic equations is formulated in a general form as follows:

$$\dot{\mathbf{x}} = \mathbf{f}(\mathbf{x}, \mathbf{y}, \mathbf{u}) \quad (1)$$

$$\mathbf{0} = \mathbf{g}(\mathbf{x}, \mathbf{y}) \quad (2)$$

where $\mathbf{x}$ is the vector of the state variables, $\mathbf{y}$ is the vector of the algebraic variables, and $\mathbf{u}$ is the input vector. Those equations are integrated using either explicit or implicit methods [16].

Through network impedance, machine characteristics, load characteristics and transient stability controls all play their parts in system dynamic responses. For each synchronous machine i, there are two differential equations in (1), known as the swing equation:

$$\dot{\delta}_i = \omega_i - \omega_B = \Delta\omega_i \quad (3)$$

$$\frac{2H_i}{\omega_s}\frac{d\omega_i}{dt} = \frac{2H_i}{\omega_s}\frac{d\Delta\omega_i}{dt} = T_{Mi} - T_{E_i} - D_i\Delta\omega_i \quad (4)$$

T_{Mi} and T_{Ei} are mechanical and electrical torques, between which the difference results in the change of rotor angular velocity ω_i and position δ_i. H_i is the normalized inertia value $H_i = \frac{J_i(\omega_B)^2}{2S_B}$, with a MVA base S_B and rotor's actual moment of inertia J_i. Given a fixed difference between a generator's mechanical input and electrical output, rotor accelerates or decelerates faster if inertia is lower, and vice versa.

2.2. Modal Analysis

Post-contingency system responses may experience oscillations that either damp out, sustain or grow. Those oscillatory responses can be measured and analyzed to extract modal information of the system. Idea of modal analysis is to approximate a signal $z(t)$ by the sum of exponential functions $\hat{z}(t) = \sum_k a_k \exp(\lambda_k t)$ that could preserve the original signal's properties such as oscillation frequency and damping. $\hat{z}(t)$ is typically obtained by solving the following minimization problem for a set of sampling points [17], [18].

$$\min_{a_k, \lambda_k} \sum_{t \in \mathbb{T}} (z(t) - \hat{z}(t))^2 \quad (5)$$

The damping ratio is then calculated as $-\frac{100\sigma_k}{\sqrt{\sigma_k^2+\omega_k^2}}$, where σ_k and $\omega_k = 2\pi f_k$ are the real and imaginary parts of the eigenvalue λ_k associated with each mode k. f_k is mode k oscillation frequency. For each mode, unique relationships among the four parameters are: a) when damping of a mode increases, the real part σ_k changes from positive to negative, and vice versa; b) when frequency of a mode increases, the imaginary part ω_k increases, and vice versa.

In this paper, the variable projection method (VPM) is used to determine the characteristic modes observed from time series analysis [19]. We use oscillation frequency and damping ratio as metrics to analyze the locational impacts of inertia on system oscillation modes.

3. Preliminary Studies

In this section, we apply a simple, straightforward 138-kV test system with three generators for illustrating resource inertia's locational impacts on system oscillation and damping behavior.

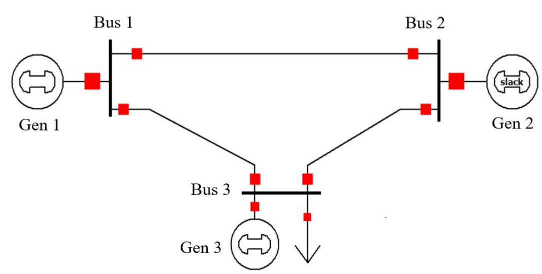

Fig. 1: Oneline diagram of a three-bus test system

3.1. Simulation Setup and Results

The three-bus test system as shown in Fig.1 supplies a load connected to bus 3. Each bus is connected to a generator. A balanced 3-phase fault is applied to bus 1 at 1 second and cleared 0.01 seconds later. We reduce the inertia of gen 3 by amounts from 0 MWs to 300 MWs in increment of 100 MWs (Case 1)[1]. Fig.2 shows the rotor speeds of generators at buses 1 and 3 in Case 1. For comparisons, Case 2 reduces the inertia of gen 1 by amounts from 0 MWs to 300 MWs in increment of 100 MWs. The rotor speeds of generators at buses 1 and 3 in Case 2 are displayed in Fig.3.

1. Inertia is often expressed in unit of second on the machine MVA base that varies by generator. Thus, we express inertia in MWs (= MVA base × inertia in s) for convenient comparisons among different generators. For instance, given a base of 100 MVA, an inertia of 1 s is equivalent to an inertia of 100 MWs.

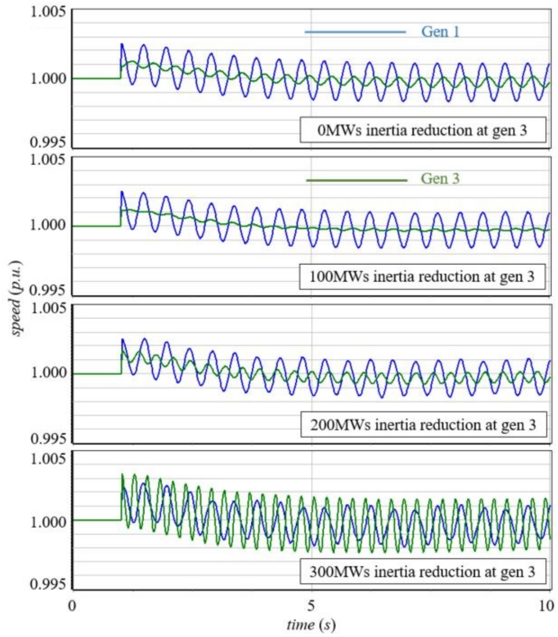

Fig. 2: Simulation results of a bus fault event on the three-bus test system with varying inertia of gen 3

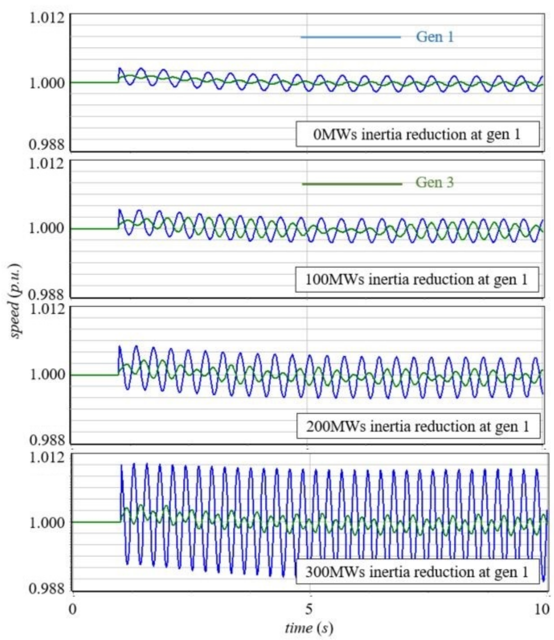

Fig. 3: Simulation results of a bus fault event on the three-bus test system with varying inertia of gen 1

3.2. Discussion

The inertia reduction at each generator significantly changes the local oscillation magnitude. In Case 1, the local oscillation magnitude at bus 3 becomes smaller first and then increases as the gen 3's inertia is reduced. Meanwhile, the local oscillation frequency at bus 3 has similar behavior. Rather, gen 1's inertia reduction in Case 2 always enlarges the local oscillation magnitude and frequency at bus 1. Those results indicate that local inertia has large effects on local oscillation modes. We also note that the inertia reduction at each generator also impacts its nearby generator's oscillation. In Fig.2 (Fig.3), inertia reduction at bus 3 (1) slightly increases the oscillation magnitude of gen 1 (3). Furthermore, with 300-MWs inertia reduction in Case 2, more than one oscillation mode are observed for the gen 3 rotor speed.

To provide insights into changes in oscillation modes, Table 1 displays the modal analysis results on the three-bus test system with varying inertia. The original system oscillates at 2.1 Hz. We observe one slow mode (2.106 Hz with damping ratio of 0.127 %) and one fast mode (2.122 Hz with damping ratio of 0.087 %). Inertia reduction in Case 1 slightly changes the slow oscillation mode, and significantly speed up and amplify the fast oscillation. In contrast, the slow oscillation mode oscillates faster with a higher magnitude and the fast one changes little, as inertia in bus 1 is reduced. Furthermore, in Case 2, 300-MWs inertia reduction at Gen 1 results in unstable system frequency with a negative damping ratio. This mode at 3.648 Hz is also observed at Gen 3 rotor speed, as shown in the bottom figure of Fig.3.

Table 1: Modal analysis results on the three-bus test system with varying inertia

Case		1		2	
Mode	Inertia Change(MWs)	Freq (Hz)	Damping Ratio (%)	Freq (Hz)	Damping Ratio (%)
Slow	0	2.106	0.127	2.106	0.127
	100	2.107	0.076	2.328	0.055
	200	2.108	0.092	2.716	0.012
	300	2.107	0.085	3.648	-0.035
Fast	0	2.122	0.087	2.122	0.087
	100	2.348	0.065	2.126	0.083
	200	2.755	0.055	2.125	0.096
	300	3.371	0.049	2.122	0.108

Both cases demonstrate that inertia contributes to the system oscillation modes. The locational dependence of resource inertia's impacts on power system oscillation modes is also observed in this small-test case system. In the remaining of this paper, we focus our simulations studies on system dynamic responses using a synthetic large-scale test system.

4. Illustrative Studies using Synthetic Network Models

To provide insightful and realistic results, we perform more simulations using synthetic network models that are built by applying statistics summarized from actual system models and data available to public [11]–[13]. Those synthetic models available at [14] are entirely fictitious, but are able to capture structural and functional features of actual power grids.

4.1. Simulation Setup

This section adopts a 2000-bus synthetic network - ACTIVSg2k - on the Electric Reliability Council of Texas (ERCOT) footprint, as shown in Fig.4. Given a load level set to 67 GW, the system has a total inertia of 390 GWs from online generation units. This test system has eight areas. Table. 2 summarizes the total resource inertia of online units in each area. We consider three regions (R1 with COAST, R2 with SCENT and SOUTH, and R3 with NORTH, NCENT and FWEST) in the following case studies. R2 and R3 have similar total regional inertia, which is lower than that of R1.

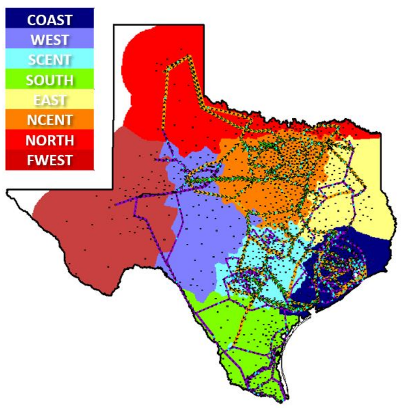

Fig. 4: Eight areas in the ACTIVSg2k model

Table 2: Total resource inertia of online generation units of each area in the synthetic network dynamic model

Area Name	COAST	EAST	FWEST	WEST
Inertia (MWs)	153548	26638	8318	301
Area Name	NCENT	NORTH	SCENT	SOUTH
Inertia (MWs)	83090	11626	74521	34557

4.2. Case Study Set I

Table.3 provides details on Case Set I. Each subset in Set I has a local oscillation caused by a few generators, defined as a set O. Set I aims to study how local oscillations are impacted by the amount and location of inertia of generator set O (local inertia), nearby generators in the same region as O (nearby inertia) and ones far away from O (remote inertia). In both Case Sets I.1 and I.2, Case (a) performs studies using the original system. Cases (b) and (c) reduce remote inertia in one region by 50 GWs. Nearby inertia that does not include that of generators in O is reduced by 50 GWs in Case (d). Inertia of generators in O is decreased by 50 % in Case (e).

Table 3: Case Set I Detail

Case	I.1	I.2
Event Type	three-phase bus fault	line outage
Event Location	R1	R3
Oscillation Origin	R3	R1
Local Inertia	O_1	O_2
Nearby Inertia	R3 (O_1 excluded)	R1 (O_2 excluded)
Remote Inertia	R1 & R2	R2 & R3

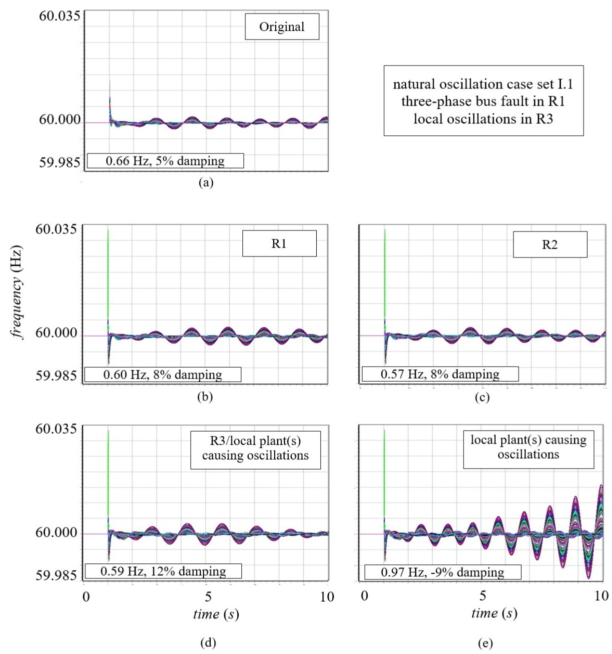

Fig. 5: Simulated bus frequencies in Case Set I.1

Case Set I.1 considers a three-bus fault in R1. As shown in Fig.5(a), the original system experiences a 0.66-Hz local oscillation of the generator set O_1 in R3. Fig.5(b) and (c) present bus frequencies with a 50-GWs regional inertia reduction in R1 and R2, respectively. Results in Fig.5(d) are obtained after R3 regional inertia of online generators (O_1 excluded) is reduced by 50 GWs, while those in Fig.5(e) are obtained after only inertia of generator set O_1 is reduced by 50%. Oscillation frequency and damping ratio are also displayed in Fig.5(a)-(e). Nearby and remote inertia reduction slows down this oscillation and improves its damping performance. However, impacts of both nearby and remote inertia reduction on this local oscillation are trivial. In contrast, the local inertia reduction significantly worsens this local oscillation. Due to decreased local inertia, this mode oscillates faster and its damping ratio becomes negative, which causes an unstable system condition.

In Case Set I.2, after a transmission line in R3 is open, this test system experiences a 1.24-Hz local oscillation caused by the generator set O_2 in R1. Similar to case design in Set I.1, Case I.2.b and Case I.2.c study the impact of remote inertia, by running simulation with a 50-GWs regional inertia reduction in R2 and R3, respectively. Case I.2.d reduces the R1 regional inertia of online generators (O_2 excluded) by 50 GWs, and Case I.2.e decreases inertia only of generators in O_2 by 50%. Comparing with Case Set I.1, we observe very different results in Case Set I.2. The well-damped oscillations in Fig.6(e) shows that local inertia reduction significantly improves local oscillation. Nearby and remote inertia reduction significantly worsen this oscillation. In particular, oscillations in Cases I.2.b-I.2.d are growing with negative damping ratios. This is because the generators near the local oscillation origin are less capable to prevent the oscillation from spreading over the network and disturbing the network as their inertia is reduced.

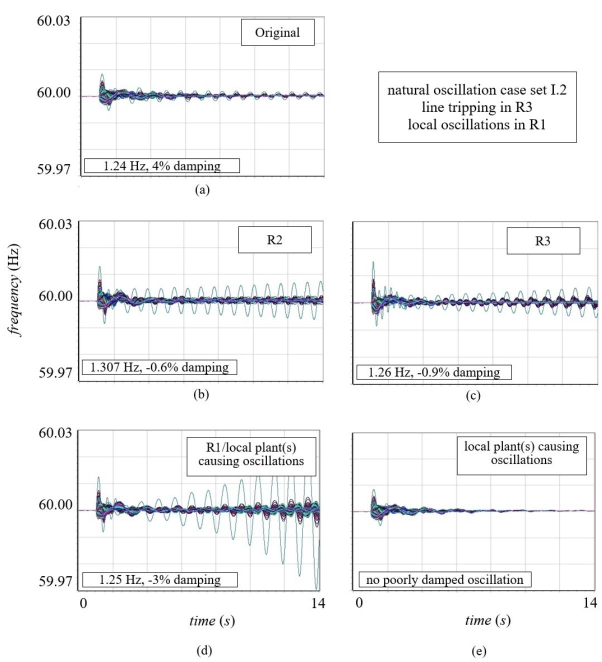

Fig. 6: Simulated bus frequencies in Case Set I.2

Both case sets indicate an important role of local inertia in the local oscillations. Local inertia reduction may largely deteriorate or alleviate oscillations. Decreased nearby and remote inertia typically worsen local oscillations, and its severeness varies by location. Furthermore, the locational variation in the impacts of local inertia, nearby inertia and remote inertia is also depending on the current system operating condition.

4.3. Case Study Set II

To further study the effects of the inertia and its location on system oscillation modes, we perform sensitivity studies with a forced oscillation to trigger system oscillations. In Case Set II, we subject this system to a 1-Hz forced oscillation for a generator in R1. For each region, we proportionally reduce the inertia of each unit in that region such that the reduction in the regional total inertia varies from 0 MWs to 50,000 MWs in increment of 5,000 MWs. For comparisons, we perform the same simulations using the synthetic model with the reduced total inertia of the system varying from 0 MWs to 50,000 MWs in increment of 5,000 MWs (reference case 0).

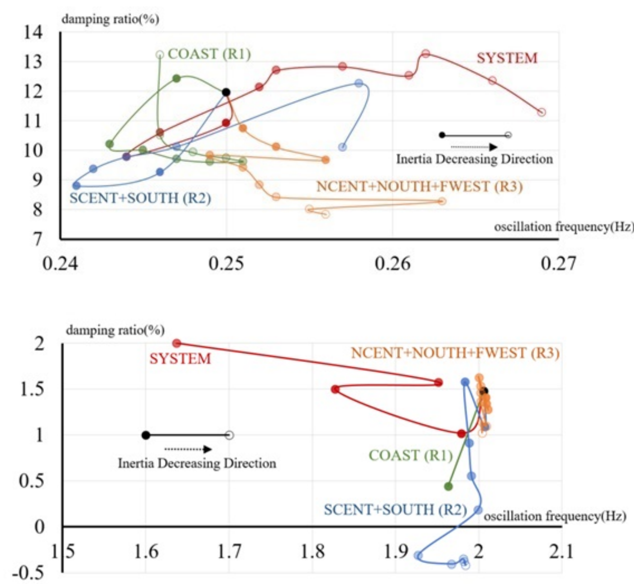

Fig. 7: Modal analysis results in Case Set II

Fig.7 displays the change of oscillation frequency and damping ratio with respect to the reduction in regional inertia. We note that the inertia reduction in different regions have distinguishable impacts on the system modes. In particular, inertia reduction in R2 causes the 2-Hz mode moving from poorly damping to negatively damping. We note discontinuity in oscillation mode change as the inertia reduces. Some modes always exist from 0 GWs all the way up to 50 GWs of inertia reduction, while other modes only show up in a particular period of inertia reduction. This is because the VPM is a measurement-based approach and hence the modes with a trivial magnitude are not observable for a certain period of inertia reduction. For instance, when the regional inertia in R1 is reduced by more than 15 GWs, the 2.1-Hz mode vanishes.

In summary, we carried out several studies to reveal the sensitivity of modal analysis results with respect to the inertia reduction in different regions. Simulation results demonstrate that the impacts of inertia on system oscillation behavior vary by inertia's location.

5. Conclusion

In this paper, both a small-scale test system and a large-scale synthetic dynamic model were used to study the inertia's impacts on system oscillation modes. Natural oscillation modes were triggered by either a three-phase bus fault, a transmission line outage or a forced oscillation. We performed time-domain simulations and modal analysis, and observed the locational dependence of impacts of inertia. As such, inertia should be an important factor to be taken into consideration during activities related to power system transient stability.

Replacement of conventional units by light- or zero-inertia units will be considered to study the locational impacts of inertia. Both frequency/RoCoF ranges and oscillation modes should be considered as essential metrics for assessment of system dynamic responses. Given the location-dependent values and impacts of inertia, it is also of interest to construct a comprehensive market simulation tool with integration of transient stability constraints. We will report these studies in future work.

Acknowledgment

The authors would like to thank the U.S. Department of Energy Consortium for Electric Reliability Technology Solutions (CERTS) for their support in this research.

References

[1] NERC, "Balancing and frequency control," January 2011. [Online]. Available: http://www.nerc.com/docs/oc/rs/NERC\%20Balancing\%20and\%20Frequency\%20Control\%20040520111.pdf.

[2] ——, "Frequency response initiative report," October 2012. [Online]. Available: http://www.nerc.com/docs/pc/FRI_Report_10-30-12_Master_w-appendices.pdf.

[3] D. Gautam, V. Vittal, and T. Harbour, "Impact of increased penetration of dfig-based wind turbine generators on transient and small signal stability of power systems," *IEEE Transactions on Power Systems*, vol. 24, no. 3, pp. 1426–1434, Aug 2009.

[4] J. McLoughlin, Y. Mishra, and G. Ledwich, "Estimating the impact of reduced inertia on frequency stability due to large-scale wind penetration in australian electricity network," in *Power Engineering Conference (AUPEC), 2014 Australasian Universities*, Sept 2014, pp. 1–6.

[5] T. Xu, A. B. Birchfield, K. S. Shetye, and T. J. Overbye, "Creation of synthetic electric grid models for transient stability studies," *accepted by 2017 IREP Symposium Bulk Power System Dynamics and Control*, 2017.

[6] NERC, "Reliability guideline - forced oscillation monitoring & mitigation," June 2017. [Online]. Available: http://www.nerc.com/pa/RAPA/rg/ReliabilityGuidelines/Reliability_Guideline_-_Forced_Oscillations_-_2017.pdf

[7] T. Xia, Y. Zhang, L. Chen, Z. Yuan, P. N. Markham, Y. Ye, and Y. Liu, "Phase angle-based power system inter-area oscillation detection and modal analysis," *European Transactions on Electrical Power*, vol. 21, no. 4, pp. 1629–1639, 2011.

[8] S. Eftekharnejad, V. Vittal, G. T. Heydt, B. Keel, and J. Loehr, "Impact of increased penetration of photovoltaic generation on power systems," *IEEE Transactions on Power Systems*, vol. 28, no. 2, pp. 893–901, May 2013.

[9] ——, "Small signal stability assessment of power systems with increased penetration of photovoltaic generation: A case study," *IEEE Transactions on Sustainable Energy*, vol. 4, no. 4, pp. 960–967, Oct 2013.

[10] R. Witzmann, "Damping of interarea oscillations in large interconnected power systems," in *International Conference on Power Systems Transients*, 2001.

[11] A. B. Birchfield, K. M. Gegner, T. Xu, K. S. Shetye, and T. J. Overbye, "Statistical considerations in the creation of realistic synthetic power grids for geomagnetic disturbance studies," *IEEE Transactions on Power Systems*, vol. 32, no. 2, pp. 1502–1510, March 2017.

[12] A. B. Birchfield, T. Xu, K. M. Gegner, K. S. Shetye, and T. J. Overbye, "Grid structural characteristics as validation criteria for synthetic networks," *IEEE Transactions on Power Systems*, vol. PP, no. 99, pp. 1–1, 2016.

[13] T. Xu, A. B. Birchfield, K. M. Gegner, K. S. Shetye, and T. J. Overbye, "Application of large-scale synthetic power system models for energy economic studies," in *Hawaii International Conference on System Sciences (HICSS-50)*, Jan 2017, pp. 3123–3129.

[14] "Electric Grid Test Case Repository - Synthetic Electric Grid Cases." [Online]. Available: https://electricgrids.engr.tamu.edu/

[15] G. Rogers, *Power System Oscillation*. New York, NY, USA: 2000, 2010.

[16] J. D. Glover, M. S. Sarma, and T. Overbye, *Power System Analysis and Design*, 5th ed. Cengage Learning, 2011.

[17] P. Kundur, *Power System Stability and Control*. New York, NY: McGraw-Hill, 1994.

[18] P. Sauer and M. Pai, *Power System Dynamics and Stability*. Champagin, IL: Stripes Publishing L.L.C., 1997.

[19] J. G. A. Borden, B.C. Lesieutre, "Power system modal analysis tool developed for industry use," in *Proc. 2013 North American Power Symposium*, Sept 2013.

Ti Xu (S'12) received the B.S. degree in 2011 from Tsinghua University, Beijing, P.R.C.. He received the M.S. and Ph.D. degrees from the University of Illinois at Urbana-Champaign, Urbana, IL, USA, in 2014 and 2017. He is currently a postdoctoral researcher in Electrical and Computer Engineering at the Texas A&M University, College Station, TX, USA.

Wonhyeok Jang (S'10) received the B.S. and M.S. degrees in Electrical Engineering from Sungkyunkwan University, Seoul, Korea. He received the Ph.D. degree in 2017 from the University of Illinois at Urbana-Champaign, Urbana, IL, USA. He is currently a postdoctoral researcher in Electrical and Computer Engineering at the Texas A&M University, College Station, TX, USA.

Thomas J. Overbye (S'87−M'92−SM'96−F'05) received the B.S., M.S., and Ph.D. degrees in electrical engineering from the University of Wisconsin-Madison, Madison, WI, USA. He is currently the TEES Distinguished Research Professor in Electrical and Computer Engineering at the Texas A&M University, College Station, TX, USA.